Available online at www.sciencedirect.com
SCIENCE DIRECT®
Journal of Sound and Vibration 262 (2003) 845–864
JOURNAL OF SOUND AND VIBRATION
www.elsevier.com/locate/jsvi

Non-linear dynamics and control of chaos for a rotational machine with a hexagonal centrifugal governor with a spring

Zheng-Ming Ge*, Ching-I Lee

Department of Mechanical Engineering, National Chiao Tung University, 1001 Ta Hsuei Road, Hsinchu 30050, Taiwan, ROC

Received 17 March 2000; accepted 16 October 2000

Abstract

The dynamic behaviors of the rotational machine with a hexagonal centrifugal governor which is subjected to external disturbance are studied in the paper. The Lyapunov direct method is applied to obtain conditions of stability of the equilibrium points of system. By applying numerical results, phase diagrams, power spectrum, Poincaré maps, and Lyapunov exponents are presented to observe periodic and chaotic motions. The effect of the parameter changes in the system can be found in the bifurcation and parametric diagrams. Finally, eight methods are used to control chaos effectively.

1. Introduction

During the past two decades, a large number of studies have shown that chaotic phenomena are observed in many physical systems that possess non-linearity [1–3]. The centrifugal governor is a device that automatically controls the speed of an engine and prevents the damage caused by a sudden change of load torque. It plays an important role in many rotational machines such as diesel engine, steam engine and so on. When an engine system is subjected to external disturbances, the speed of the engine will vary. In order to diminish the change of engine speed, and avoid the chaotic motion emerging in the operational process of the engine, in this paper the regular and chaotic dynamics of a rotational machine with centrifugal governor that is assumed to have the periodic external disturbance is studied in detail.

The aim of this paper is to present the detailed dynamics of this mechanical system. A lot of modern techniques are used in analyzing the deterministic non-linear system behavior. Both

*Corresponding author. Tel.: 886-3-5712121; fax: 886-3-5720634.
E-mail address: zmg@cc.nctu.edu.tw (Z.-M. Ge).

0022-460X/03/$ - see front matter
doi:10.1016/S0022-460X(03)00092-0

analytical and computational methods such as phase diagrams, power spectrum, Poincaré maps, Lyapunov exponents, bifurcation diagram and parametric diagram are employed to obtain the characteristics of the non-linear system. Finally, attention is shifted to the control chaos. For this purpose, several methods, i.e., the addition of constant motor torque, the addition of periodic torque, using periodic impulse input as a control torque, the delayed feedback control, external force feedback control, bang–bang control, optimal control and adaptive control algorithm are used.

2. Equations of motion

The rotational machine with centrifugal governor is depicted in Fig. 1. Some basic assumptions for the system are:

1. neglecting the mass of the rods and the sleeve;
2. viscous damping in rod bearing of the fly-ball is represented by damping constant c.

From Fig. 1, the kinetic and potential energies of the system are written as follows:

$$T = 2 \times \{\tfrac{1}{2} m[(r + l \sin \phi)^2 \eta^2 + l^2 \dot{\phi}^2]\} = m\eta^2 (r + l \sin \phi)^2 + ml^2 \dot{\phi}^2,$$

$$V = 2kl^2 (1 - \cos \phi)^2 + 2mgl(1 - \cos \phi),$$

where l, m, r and ϕ represent the length of the rod, the mass of fly ball, the distance between the rotational axis and the suspension joint, and the angle between the rotational axis and the rod. It is easy to obtain the Lagrangian

$$L = T - V = m\eta^2 (r + l \sin \phi)^2 + ml^2 \dot{\phi}^2 - 2kl^2 (1 - \cos \phi)^2 - 2mgl(1 - \cos \phi).$$

Then using Lagrange equation, the equation of motion for the governor can be derived as follows:

$$2[ml^2 \ddot{\phi} - mrl\eta^2 \cos \phi - (2k + m\eta^2) l^2 \sin \phi \cos \phi + (2kl + mg) l \sin \phi] = -c\dot{\phi}, \tag{2.1}$$

where c is the damping coefficient.

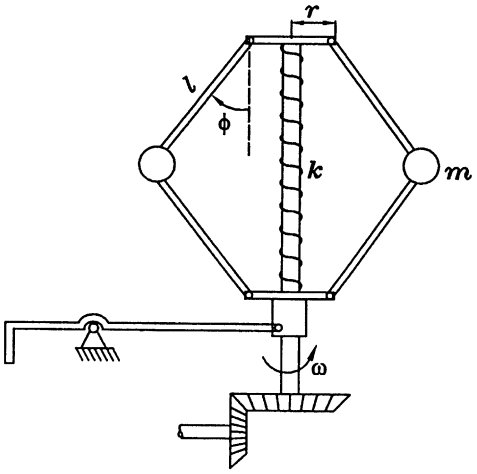

Fig. 1. Physical model of the system.

For the rotational machine the net torque is the difference between the torque Q produced by the engine and the load torque Q_L, which is available for angular acceleration, that is,

$$J\frac{\mathrm{d}\omega}{\mathrm{d}t} = Q - Q_L, \tag{2.2}$$

where J is the moment of inertia of the machine. As the angle ϕ varies, the position of control valve which admits the fuel is also varied. The dynamical Eq. (2.2) can be written in the form

$$J\dot{\omega} = \gamma\cos\phi - \beta, \tag{2.3}$$

where $\gamma > 0$ is a proportionally constant and β is an equivalent torque of the load. Eq. (2.3) is the second differential equation of motion for the system.

Usually, the governor is geared directly to the output shaft such that its speed of rotation is proportional to the engine speed, i.e., $\eta = n\omega$. The operation of the fly-ball governor can be briefly described as follows. At first, set the speed of engine at ω_0. If the speed of engine drops down, the centrifugal force acting on the fly-ball would decrease, thus the control valve of fuel will open wider. When more fuel is supplied, the speed of the engine increases until equilibrium is again reached. Similarly, if the speed rises up, the fuel supply is reduced and the speed decreases until ω_0 is recovered.

Change time scale $\tau = \Omega_n t$, Eqs. (2.1) and (2.3) can be written in non-dimensional form

$$\begin{gathered}\dot{\phi} = \varphi,\\ \dot{\phi} = d\omega^2\cos\phi + (e + p\omega^2)\sin\phi\cos\phi - \sin\phi - b\varphi,\\ \dot{\omega} = q\cos\phi - F,\end{gathered} \tag{2.4}$$

where

$$q = \frac{\gamma}{J\Omega_n},\quad F = \frac{\beta}{J\Omega_n},\quad d = \frac{n^2 mr}{2kl + mg},\quad e = \frac{2kl}{2kl + mg},$$
$$p = \frac{n^2 ml}{2kl + mg},\quad b = \frac{c}{2ml^2\Omega_n},\quad \Omega_n = \sqrt{\frac{2kl + mg}{ml}},$$

and the dot presented the derivative with respect to τ, φ is $\mathrm{d}\phi/\mathrm{d}\tau$. Hence, the dynamics of the system of rotational machine with fly-ball governor is described by a three-dimensional autonomous system.

3. Stability analysis by Lyapunov direct method

Find the equilibrium points of the system and determine the stability of them. These equilibrium points can be found from Eq. (2.4) as $p_e = (\phi_0,\ 0,\ \omega_0)$ with

$$\cos\phi_0 = \frac{F}{q},\quad \omega_0^2 = \frac{(q - eF)\sqrt{q^2 - F^2}}{F(dq + p\sqrt{q^2 - F^2})}.$$

Add slight disturbances x, y, z to the equilibrium point $(\phi_0, 0, \omega_0)$

$$\phi = \phi_0 + x, \quad \varphi = y, \quad \omega = \omega_0 + z. \tag{3.1}$$

Substituting Eq. (3.1) into Eq. (2.4), and expanding to Taylor series, it becomes

$$\begin{aligned} \dot{x} &= y, \\ \dot{y} &= -Ax - By + Cz + \cdots, \\ \dot{z} &= -Dx + \cdots, \end{aligned} \tag{3.2}$$

where

$$\begin{aligned} A &= \{\omega_0^2\,[dq\sqrt{q^2 - F^2} - p(2F^2 - q^2)] + qF - e(2F^2 - q^2)\}/q^2, \\ B &= b, \\ C &= 2\omega_0 F(dq + p\sqrt{q^2 - F^2})/q, \\ D &= \sqrt{q^2 - F^2}. \end{aligned}$$

and the terms higher than one degree have not been written down. Let $q > F > 0$, then $A > 0$, $B > 0$, $C > 0$ and $D > 0$.

First, asymptotical stability of the origin of Eq. (3.2) can be studied by using Lyapunov direct method. Construct the quadratic Lyapunov function candidate in the form

$$V(x, y, z) = A_{11}x^2 + A_{22}y^2 + A_{33}z^2 + 2A_{12}xy + 2A_{13}xz - 2yz.$$

Let p_i $(i = 1, 2, 3)$ be the principal minor determinants of the characteristic matrix of the quadratic form, then

$$\begin{aligned} p_1 &= A_{11}, \\ p_2 &= A_{11}A_{22} - A_{12}^2, \\ p_3 &= A_{11}A_{22}A_{33} - 2A_{12}A_{13} - A_{11} - A_{22}A_{13}^2 - A_{33}A_{12}^2. \end{aligned}$$

By Sylvester's criterion [4], V is positive definite if and only if that all p_i are positivee:

$$\begin{aligned} A_{11} &> 0, \\ A_{11}A_{22} - A_{12}^2 &> 0, \\ A_{11}A_{22}A_{33} - 2A_{12}A_{13} - A_{11} - A_{22}A_{13}^2 - A_{33}A_{12}^2 &> 0. \end{aligned}$$

The derivative of V with respect to τ is given by

$$\begin{aligned} \dot{V} = &-2(AA_{12} + DA_{13})x^2 + (2A_{12} - 2CA_{22})y^2 - 2Bz^2 + (2A_{11} - 2AA_{22} - 2CA_{12} + 2D)xy \\ &+ (2A + 2BA_{12} - 2DA_{33})xz + (2C + 2A_{13} + 2BA_{22})yz + \ldots\ . \end{aligned}$$

Now, it is necessary to choose A_{11}, A_{22}, A_{33}, A_{12} and A_{13} such that V and $-\dot{V}$ are positive definite. Let

$$A_{11} = \frac{AC + A^2C + B^2C + BC^2D + B^3D + CD^2}{AB - CD},$$

$$A_{22} = \frac{C + AC + BD}{AB - CD},$$

$$A_{33} = \frac{A^2B + BC^2 - ACD + C^3D + B^2CD}{ABD - CD^2},$$

$$A_{12} = \frac{BC + B^2D + C^2D}{AB - CD},$$

$$A_{13} = \frac{C^{2+}AB^2\_AC^2}{CD - AB}.$$

Then

$$\dot{V}(x, y, z) = -B(x^2 + y^2 + z^2) + \cdots$$

is negative definite. By Sylvester's theorem, the sufficient condition for V to be positive definite is founded:

$$AB > CD,$$

i.e.,

$$b > \frac{2qF\,[d\sqrt{q^2 - F^2} + p(q^2 - F^2)]}{\omega_0[d\sqrt{q^2 - F^2} - p(2F^2 - q^2)] + qF - e(2F^2 - Q^2)}. \tag{3.3}$$

From the Lyapunov asymptotic stability theorem, we conclude that the origin is asymptotically stable. Furthermore. The result is the same as analysis by a linearized system.

For the given range for disturbance ε, we can find the allowable range for the initial disturbances Ω by the Lyapunov function. Let

$$R^2 = x^2 + y^2 + z^2.$$

Using the method of Lagrange's multiplier, we form Lagrange's function $L = R^2 + \lambda V$. From

$$\frac{\partial L}{\partial x} = 0, \quad \frac{\partial L}{\partial y} = 0, \quad \frac{\partial L}{\partial z} = 0,$$

we have

$$\lambda_1 = \frac{-u_2}{3u_3} - \frac{\sqrt[3]{2}(-u_2^2+3u_1u_3)}{(-2u_2^3+9u_1u_2u_3-27u_3^2+\sqrt{4(-u_2^2+3u_1u_3)^3+(-2u_2^3+9u_1u_2u_3-27u_3^2)^2})^{1/3}} + \frac{(-2u_2^3+9u_1u_2u_3-27u_3^2+\sqrt{4(-u_2^2+3u_1u_3)^3+(-2u_2^3+9u_1u_2u_3-27u_3^2)^2})^{1/3}}{3\times\sqrt[3]{2u_3}},$$

$$\lambda_{2,3} = \frac{-u_2}{3u_3} + \frac{(1\pm\sqrt{3}\mathrm{i})(-u_2^2+3u_1u_3)}{(-2u_2^3+9u_1u_2u_3-27u_3^2+\sqrt{4(-u_2^2+3u_1u_3)^3+(-2u_2^3+9u_1u_2u_3-27u_3^2)^2})^{1/3}} - \frac{(1\mp\sqrt{3}\mathrm{i})(-2u_2^3+9u_1u_2u_3-27u_3^2+\sqrt{4(-u_2^2+3u_1u_3)^3+(-2u_2^3+9u_1u_2u_3-27u_3^2)^2})^{1/3}}{6\times\sqrt[3]{2}u_3},$$

where

$$u_1 = A_{11}+A_{22}+A_{33},$$
$$u_2 = -1+A_{11}A_{22}+A_{11}A_{33}+A_{22}A_{33}-A_{12}^2-A_{13}^2,$$
$$u_3 = -A_{11}+A_{11}A_{22}A_{33}-A_{33}A_{12}^2-2A_{12}A_{13}-A_{22}A_{13}^2.$$

When $\lambda=\lambda_1$, we have

$$x = x, y = z = 0.$$

Putting these in $V=c$, we have $x=x(c)=\pm\sqrt{c/A_{11}}$. Similarly, for $\lambda_{2,3}$ we have $x=x(c)$, $y=y(c)$, $z=z(c)$. Putting all these solutions in R^2, we obtain $R_x^2(c)$, $R_y^2(c)$, $R_z^2(c)$, of which the minimum is

$$R_{min}^2(c) = \min\{R_x^2(c), R_y^2(c), R_z^2(c)\}.$$

Taking $\varepsilon = R_{min}^2(c)$, we have the inverse function $c = R_{min}^{2^{-1}}(\varepsilon)$. Let $\Omega = R_{min}/\sqrt{3}$, then $V=c$ is inside of the hypersurface $\max\{x,y,z\}=\Omega$. So we have, for given ε,

$$\Omega = \frac{R_{min}}{\sqrt{3}}.$$

Next, the stability of the fixed point $(\phi_0, 0, -\omega_0)$ is studied. The differential equations for disturbances are

$$\begin{aligned} \dot{x} &= y, \\ \dot{y} &= -Ax - By - Cz + \cdots, \\ \dot{z} &= -Dx + \cdots, \end{aligned} \tag{3.4}$$

where A, B, C, D are the same as above.

In order to determine the instability of the origin of Eq. (3.4), the quadratic Lyapunov function candidate is assumed in the form

$$V(x,y,z) = -(A+D)x^2 - y^2 + \frac{A}{D}z^2 - (B+C)xy - yz.$$

The derivative V with respect to τ along the trajectories of system is given by

$$V = 2(BD + CD)x^2 + 2Cy^2 + 2Bz^2 + \cdots$$

which is positive definite. There exists the region $V(x, y, z) > 0$ in the neighborhood of the origin of Eq. (2.2.8). Its boundaries in the y–z plane are

$$y = \frac{-D + \sqrt{AD + D^2}}{D} z \quad \text{or} \quad y = \frac{-D - \sqrt{AD + D^2}}{D} z,$$

in the x–z plane are

$$x = \frac{-(B + C)D + \sqrt{(B + C)^2 D^2 + AD(A + D)}}{D(A + D)} z$$

or

$$x = \frac{-(B + C)D - \sqrt{(B + C)^2 D^2 + AD(A + D)}}{D(A + D)} z.$$

So, by Lyapunov instability theorem, the origin is unstable.

4. Regular and chaotic dynamics of non-autonomous system

In previous sections, the load torque is assumed to be constant for the system. Another condition can be considered. The load torque is now not constant but is represented by a constant term and a harmonic term $F + a \sin \bar{\omega} t$, where F, a, ω are constants. Denoting $\phi = x, \dot{\phi} = y, \omega = z$, Eq. (2.4) is rewritten in the form

$$\begin{aligned} \dot{x} &= y, \\ \dot{y} &= dz^2 \cos x + \tfrac{1}{2}(e + pz^2)\sin 2x - \sin x - by, \\ \dot{z} &= q \cos x - F - a \sin \bar{\omega} t, \end{aligned} \tag{4.1}$$

where $d = 0.08$, $e = 0.8$, $p = 0.04$, $F = 1.942$, $a = 0.6$, $b = 0.4$, $\omega = 1.0$.

4.1. Phase portraits, Poincaré map and power spectrum

The phase portrait is the evolution of a set of trajectories emanating from various initial conditions in the state space. When the solution reaches a steady state, the transient behavior disappears. The idea of transforming the study of continuous systems into the study of an associated discrete system was presented by Henri Poincaré. One of the many advantages of the Poincaré map is to reduce dimensions of the dynamical system. The solution of period-1 T in the phase will become one point in the Poincaré map. By using the fourth order Runge–Kutta numerical integration method, the phase plane and Poincaré map of the system, Eq. (4.1), is plotted in Figs. 2(a) and 2(b) for $q = 2.07$ and 2.14, respectively. Clearly, the motion is periodic.

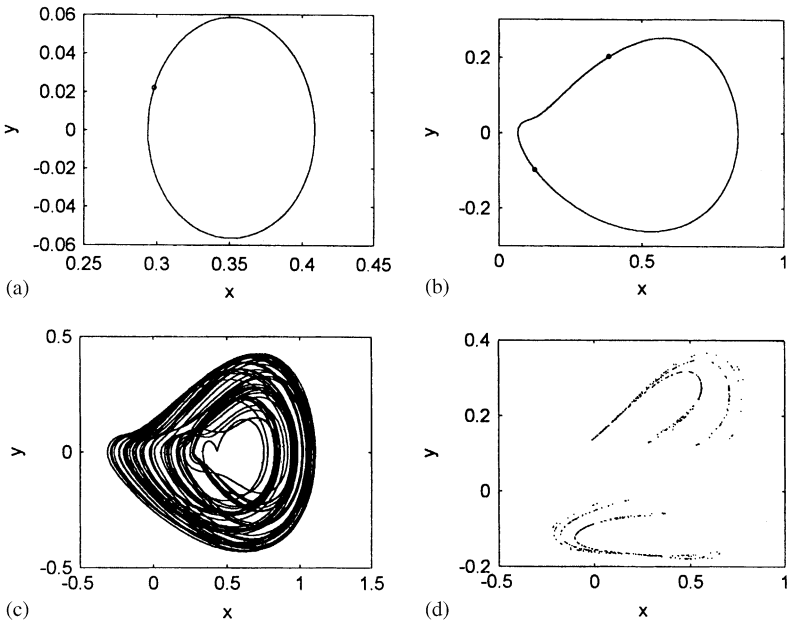

Fig. 2. (a) Phase portrait and Poincaré map for $q=2.07$, (b) $q=2.14$, (c) phase portrait for $q=2.21$, (d) Poincaré map for $q=2.21$.

But Figs. 2(c) and (d) for $q=2.21$ show the chaotic states. Because the Poincaré map is neither a finite set of points nor a closed orbit, the motion may be chaotic.

A valuable technique for the identification and characterization of the system is the power spectrum. This representation is useful for dynamical analysis. The periodic motion of the non-autonomous system is observed by the portraits of power spectrum in Fig. 3(a) for $q=2.07$. The solution of the system, is period-1T, and the power spectrum exhibits a strong peak at the forcing frequency together with super-harmonic frequencies. As the q increase, the period-1T changes to period-2T and the peak arises at one-half forcing frequency, twice of principal period in the power spectrum.

Apparently, the spectrum of the period motion only consists of discrete frequencies. As $q=2.21$ chaos occurs, the points of Poincaré map become obviously irregular. The spectrum is a broad band and the peak is still presented at the fundamental frequency shown in Fig. 3(b). The noise-like spectrum is the characteristic of a chaotic dynamical system.

4.2. *Bifurcation diagram and parametric diagram*

In the previous section, the information about the dynamics of the non-linear system for specific values of the parameters is provided. The dynamics may be viewed more completely over a range of parameter value. As the parameter is changed, the equilibrium points can be created or destroyed, or their stability can be lost. The phenomenon of a sudden change in the motion as a parameter is varied is called bifurcation, and the parameter values at which they occur are called bifurcation points.

The bifurcation diagram of the non-linear system of Eq. (4.1) is depicted in Fig. 4. It is calculated by the fourth order Runge–Kutta numerical integration and plotted against the $q \in [2.07,2.21]$ with the incremental value of q as 0.0002. At each q, the points of the Poincaré map

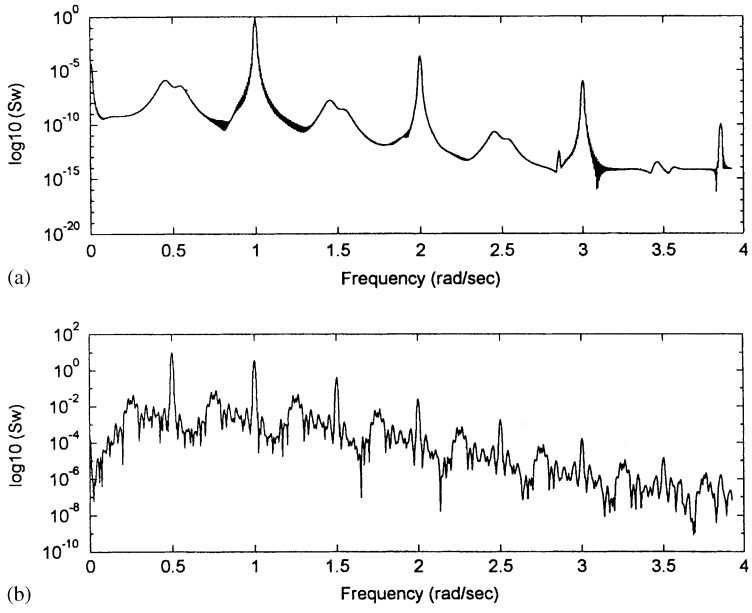

Fig. 3. Power spectrum for (a) $q=2.07$, (b) $q=2.21$.

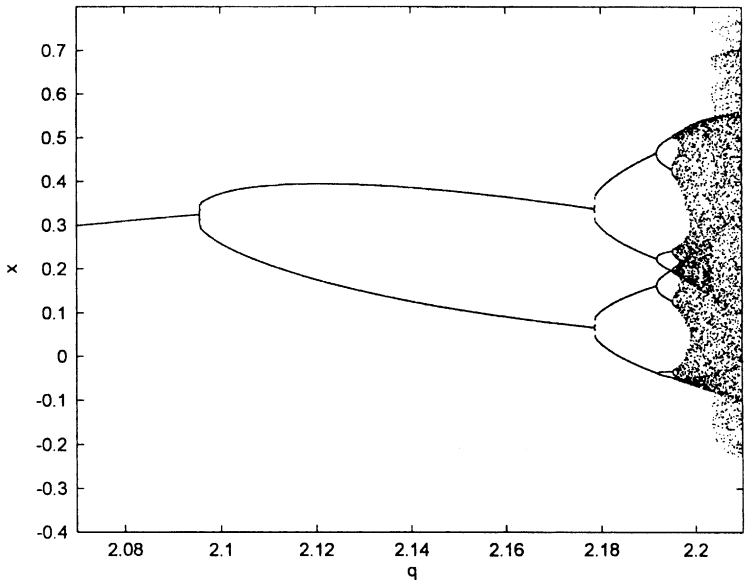

Fig. 4. Bifurcation diagram of q versus x.

in the transient state of motion are discarded. The period-doubling bifurcation first appears for $q \approx 2.095$. In this model, a sequence of period-doubling bifurcations occurs and leads to chaos as the system parameter is varied.

Further, the parameter values, damping coefficient and forcing frequency will also be varied to observe the behaviors of bifurcation of the system. By varying simultaneously any two of the three

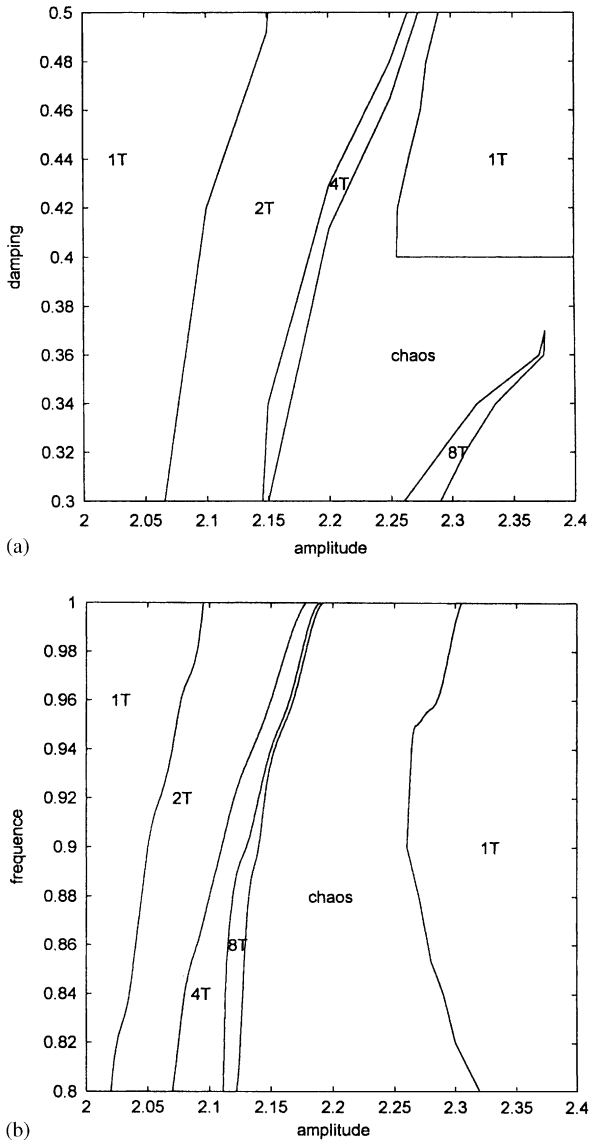

Fig. 5. Parametric diagram of (a) q versus b, (b) q versus $\bar{\omega}$.

parameters, amplitude of the external torque, damping coefficient, and forcing frequency, the parametric diagrams are described and shown as Figs. 5(a) and (b). The enriched information of the behaviors of the system can be obtained from the diagrams.

4.3. Lyapunov exponent and Lyapunov dimension

The Lyapunov exponent may be used to measure the sensitive dependence upon initial conditions. It is an index for chaotic behavior. Different solutions of a dynamical system, such as

fixed points, periodic motions, quasiperiodic motion, and chaotic motion, can be distinguished by it. If two chaotic trajectories start close to one another in phase space, they will move exponentially away from each other for small times on the average. Thus, if d_0 is a measure of the initial distance between the two starting points, the distance is $d(t) = d_0 2^{\lambda t}$. The symbol λ is called Lyapunov exponent. The divergence of chaotic orbits can only be locally exponential, because if the system is bounded, $d(t)$ cannot grow to infinity. A measure of this divergence of orbits is that the exponential growth at many points along a trajectory has to be averaged. When $d(t)$ is too large, a new 'nearby' trajectory $d_0(t)$ is defined. The Lyapunov exponent can be expressed as

$$\lambda = \frac{1}{t_N = t_0} \sum_{k=1}^{N} \log_2 \frac{d(t_k)}{d_0(t_{k-1})}.$$

The signs of the Lyapunov exponents provide a qualitative picture of a system dynamics. The criterion is

$$\lambda > 0 \quad \text{(chaotic)},$$
$$\lambda \leqslant 0 \quad \text{(regular motion)}.$$

The periodic and chaotic motions can be distinguished by the bifurcation diagram, while the quasiperiodic motion and chaotic motion may be confused. However, they can be distinguished by the Lyapunov exponent method. The Lyapunov exponents of the solutions of the non-linear dynamical system, Eq. (3.1), are plotted in Fig. 3.4 as q ranges form 2.07 to 2.21. For the system studied the sum of the four Lyapunov exponent is equivalent to the negative damping coefficient -0.4. If the value of the Lyapunov exponent is greater than zero, it is chaos, otherwise periodic solution. Observably, the chaotic motion can be found in Fig. 6 for q close to 2.2.

There are a number of different fractional-dimension-like quantities, including the information dimension, Lyapunov dimension, and the correlation exponent, etc., the difference between them is often small. The Lyapunov dimension is a measure of the complexity of the attractor. It has been developed by Kalpana and Yorke that the Lyapunov dimension d_L is introduced as

$$d_L = j + \frac{\sum_{i=1}^{j} \lambda_i}{|\lambda_{j+1}|},$$

where j is defined by the condition that

$$\sum_{i=1}^{j} \lambda_i > 0 \quad \text{and} \quad \sum_{i=1}^{j+1} \lambda_i < 0.$$

The Lyapunov dimension for a strange attractor is a non-integer number. The Lyapunov dimension and the Lyapunov exponent of the non-linear system are listed in Table 1 for the different value of q.

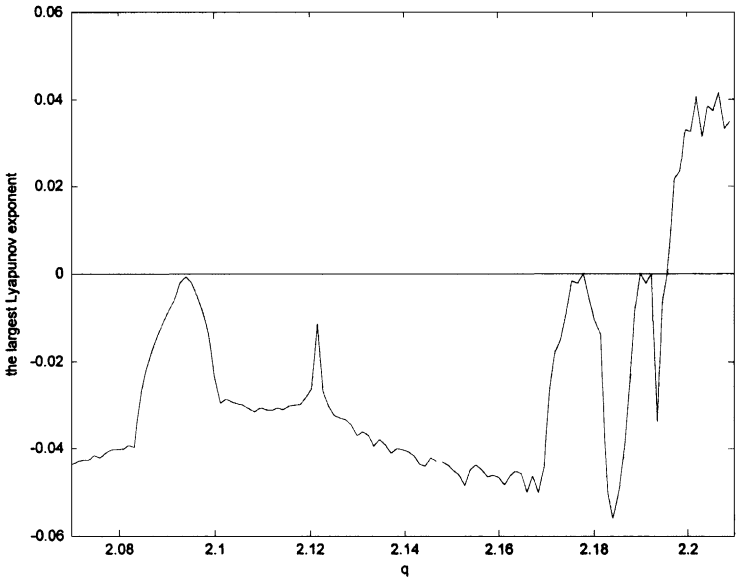

Fig. 6. The largest Lyapunov exponent for q between 2.07 and 2.21.

Table 1
Lyapunov exponent and Lyapunov dimensions of the system for different q

q	λ_1	λ_2	λ_3	λ_4	$\sum\lambda_i$	d_L	
2.07	−0.0431	0	−0.0437	−0.3132	−0.4	1	Period-1
2.14	−0.0407	0	−0.0553	−0.304	−0.4	1	Period-2
2.185	−0.0506	0	−0.0764	−0.273	−0.4	1	Period-4
2.21	0.0351	0	−0.1206	−0.3145	−0.4	2.291	Chaos

5. Controlling chaos

Several interesting non-linear dynamic behaviors of the system have been discussed in previous sections. It has been shown that the forced system exhibited both regular and chaotic motion. Usually chaos is unwanted or undesirable.

In order to improve the performance of a dynamic system or to avoid the chaotic phenomena, we need to control a chaotic motion to become a periodic motion which is beneficial for working with a particular condition. It is thus of great practical importance to develop suitable control methods. Very recently much interest has been focused on this type of problem—controlling chaos [5,6]. For this purpose, open-loop strategies and close-loop feedback methods are used to control our system from chaos to order.

5.1. Controlling chaos by addition of constant motor torque

Interestingly, one can even add just a constant term to control or quench the chaotic attractor to a desired periodic one in a typical non-linear non-autonomous system. In practice, An external

input u is a torque on the axis of rotational machine. Eq. (4.1) can be rewritten as

$$\begin{aligned} \dot{x} &= y, \\ \dot{y} &= dz^2 \cos x + \tfrac{1}{2}(e + pz^2)\sin 2x - \sin x - by, \\ \dot{z} &= q \cos x - F - a \sin \bar{\omega} t + u. \end{aligned} \tag{5.1}$$

It ensures effective control in a very simple way. In order to understand this simple controlling approach in a better way, this method is applied to system (5.1) numerically. We add the constant motor torque $u = T$ into the third equation of Eq. (5.1).

In the absence of the constant motor torque, the system exhibits chaotic behavior under the parameter condition, $q = 2.21$.

If one considers the effect of the constant motor torque T by increasing it from zero upwards, the chaotic behavior is then altered. In Fig. 7, the bifurcation diagram is shown. It is clear that the system returns to regular motion, when the constant motor torque T is great t han 0.03.

5.2. Controlling chaos by the addition of periodic force

One can control system dynamics by addition of external periodic force in the chaotic state. For our purpose, the added periodic force, $u = v \sin \tilde{\omega} t$, is given, the system can then be investigated by a numerical solution, with the remaining parameter fixed. We examine the change in the dynamics of the system as a function of v for fixed $\tilde{\omega} = 2$. The bifurcation diagram is shown in Fig. 8. It presents the return of the chaotic behavior to periodic motion while the value of v increases from zero upward.

5.3. Controlling chaos by the addition of periodic impulse input

Following the sense of previous sections, another open-loop control method is given. A technique for suppressing chaos is to apply a periodic impulse input to the system [6]. Consider the system of the form (5.1) and assume that the system is controlled by a periodic impulse input

$$u = \rho \sum_{i=0}^{\infty} \delta(\tau - iT_d), \tag{5.2}$$

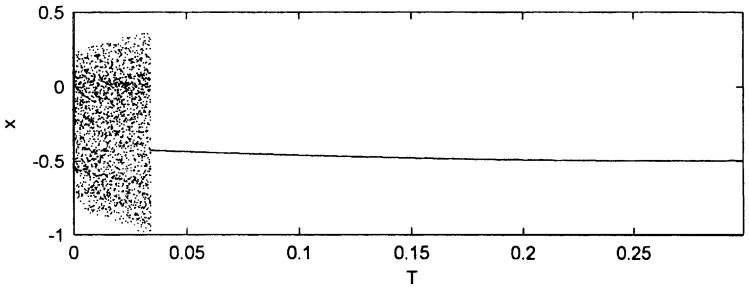

Fig. 7. Bifurcation diagram of T versus x.

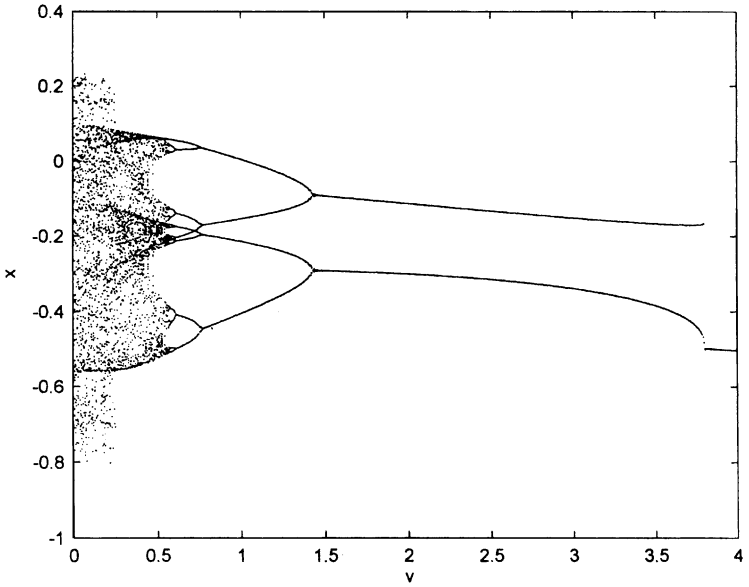

Fig. 8. Bifurcation diagram of v versus x.

where ρ is a constant impulse intensity, T_d is the period between two consecutive impulses, and δ is the standard delta function. With different values of ρ and T_d the controlled system can be stabilized at different periodic orbits. For example, if we fix the parameter $T_d = 0.01$ and adjust impulse intensity ρ, the chaotic behaviour disappears. The bifurcation diagram is shown in Fig. 9.

5.4. Controlling chaos by delayed feedback control

Let us consider a dynamic system which can be simulated by ordinary differential equations. We imagine that the equations are unknown, but some scalar variable can be measured as a system output. The idea of this method is that the difference $D(t)$ between the delayed output signal $y(t-\tau)$ and the output signal $y(t)$ is used as a control signal. In other words, we adapt a perturbation of the form [5].

$$u(t) = K[y(t-\tau) - y(t)] = KD(t). \tag{5.3}$$

Here τ is a delay time. Coosing an appropriate weight K and τ of the feedback, one can achieve the periodic state. We can control the chaotic motion to any assigned periodic motion rapidly by this method. The dependence of the bifurcation diagram on K for period-1 time delay is shown in Fig. 10.

This control is achieved by the use of the output signal, which is fed in a special form into the system. The difference between the delayed output signal and the output signal itself is used as a control signal. Only a simple delay line is required for this feedback control. To achieve the periodic motion of the system, two parameters, namely, the time of delay τ and the weight K of the feedback, should be adjusted. Compared to the simulation process, this method is more effective and applicable for the control of chaos to the rotational machine.

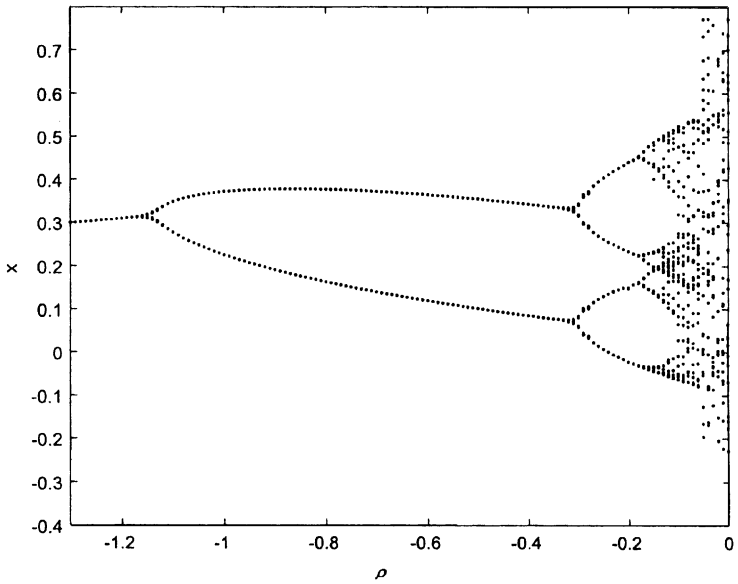

Fig. 9. Bifurcation diagram of ρ versus x.

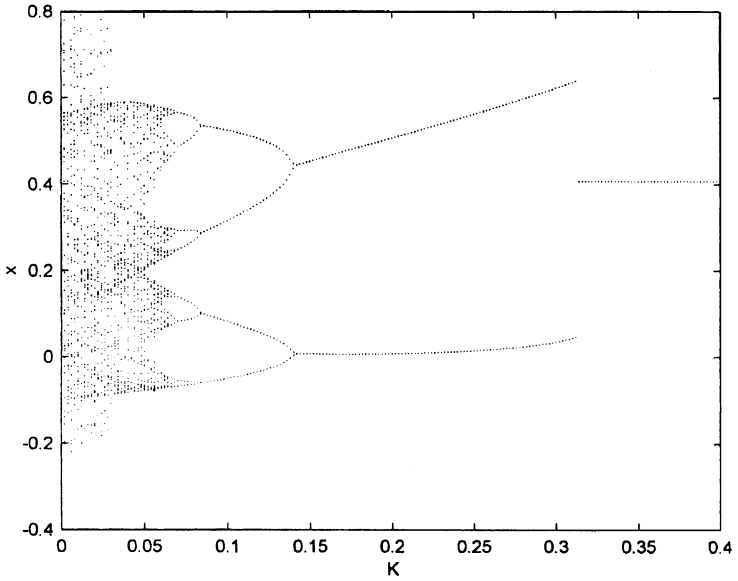

Fig. 10. Bifurcation diagram of K versus x.

5.5. Controlling chaos by adaptive control algorithm (ACA)

Recently, a simple and effective adaptive control algorithm is suggested [7], which utilizes an error signal proportional to the difference between the goal output and actual output of the

system. The error signal governs the change of parameters of the system, which readjusts so as to reduce the error to zero. This method can be explained briefly. The system motion is set back to a desired state X_s by adding dynamics on the control parameter P through the evolution equation,

$$\dot{P} = \varepsilon G(X - X_s), \tag{5.4}$$

where the function G depends on the difference between X_s and the actual output X, and ε indicates the stiffness of the control. The function G could be either linear or non-linear. In order to convert the dynamics of system (4.1) from chaotic motion to the desired periodic motion X_s, the chosen parameter q is perturbed as

$$\dot{q} = \varepsilon(X - X_S) \tag{5.5}$$

if $\varepsilon = 0.2$, the system can reach the period-1 and period-2 easily shown as Figs. 11 and 12. It is clear that the desired periodic motion can be reached by adaptive control algorithm.

5.6. Controlling chaos by bang–bang control

Define error function as follows:

$$e(t) = X(t) - X(t - T), \tag{5.6}$$

where T is the external torque frequency. Define $V(t) = e(t)^2$ which is always positive or zero,

$$\dot{V} = 2 \cdot e(t) \cdot \dot{e}(t).$$

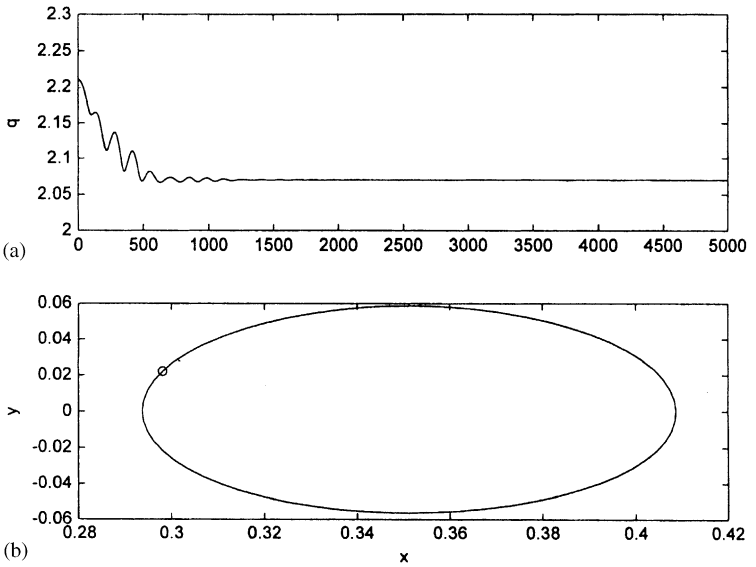

Fig. 11. (a) Parameter converge to $q = 2.07$ from chaotic motion $q = 2.21$. (b) Phase portrait and Poincaré map of controlled system.

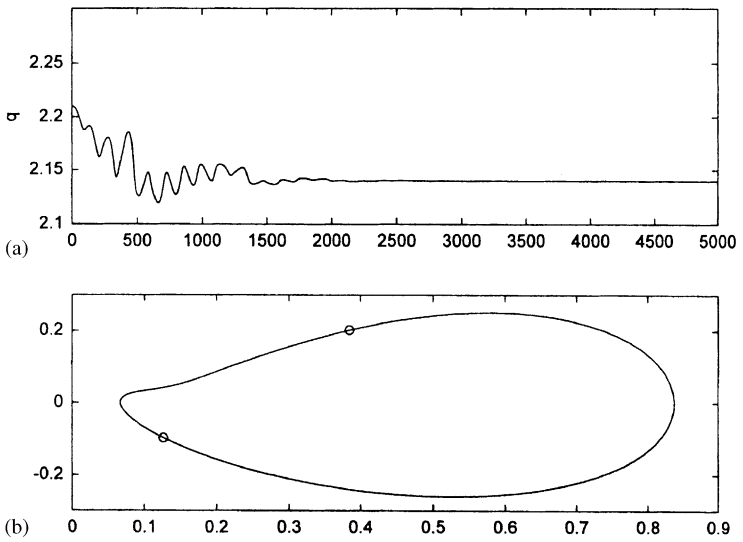

Fig. 12. (a) Parameter converge to $q=2.14$ from chaotic motion $q=2.21$. (b) Phase portrait and Poincaré map of controlled system.

if $\dot{V}<0$ then V will approach zero, i.e., $e(t)\to 0$. It means that $x(t)$ approaches $x(t-T_i)$ and the periodic behavior is achieved. The control law can be determined as follows:

$$\begin{aligned} \dot{x} &= F_1(x,y,z,t), \\ \dot{y} &= F_2(x,y,z,t), \\ \dot{z} &= F_3(x,y,z,t)+u \end{aligned} \tag{5.7}$$

if $|e(t)|\leqslant\delta, u(t)=0$ else if $|e(t)|>\delta$ then

$$u(t)=\begin{cases} -K_1|F_3(x,y,z,t)-\dot{z}(t-T)| & \text{when } e(t)>0, \\ K_1|F_3(x,y,z,t)-\dot{z}(t-T)| & \text{when } e(t)<0. \end{cases}$$

When the trajectory is close to our periodic orbit, the control signal approaches zero. Fig. 13 shows the phase portrait and Poincaré map for $K_1=0.03$.

5.7. Controlling chaos by external force control

A feedback control with a periodic external force of a special form is used in this method [5]. It is assumed that the input signal $u(t)$ disturbs only the third equation in Eq. (5.1) and

$$u(t)=K_2[y_i(t)-y(t)]=K_2D(t).$$

Here, $y(t)$ is the chaotic output signal, and $y_i(t)$ is the periodic motion of system. The difference $D(t)$ between the signal $y_i(t)$ and $y(t)$ is used as a control signal. Here K_2 is an adjustable weight of feedback. By selecting the weight K_2, we can convert chaotic behavior to periodic motion; the bifurcation diagram is shown in Fig. 14. We can control the chaotic behavior to period-1 motion

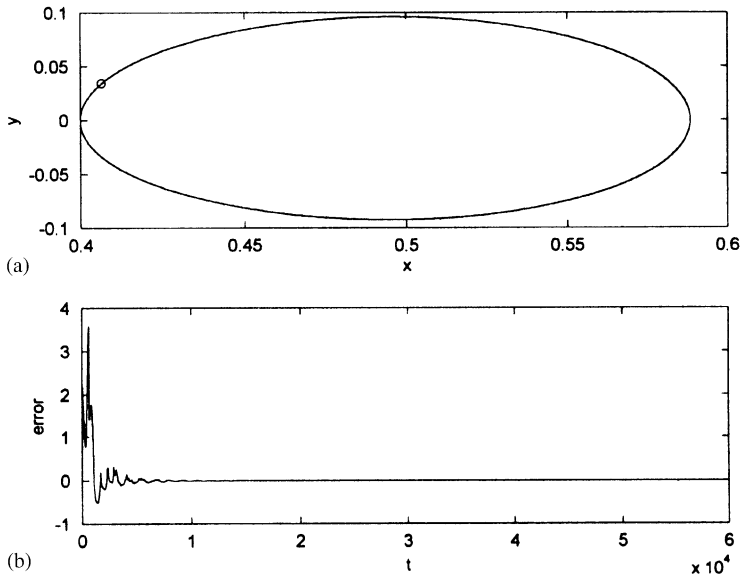

Fig. 13. (a) Phase portrait and Poincaré map of controlled system, (b) the error signal.

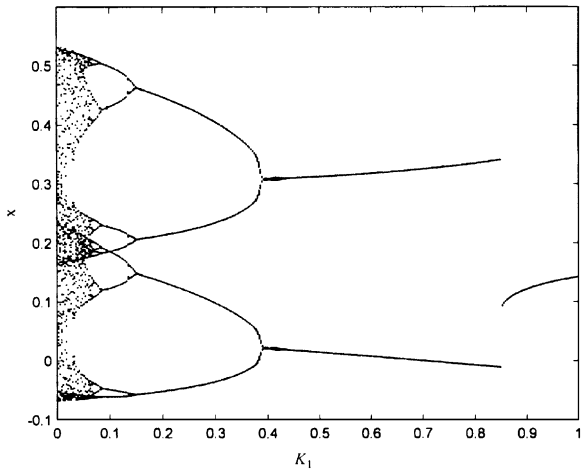

Fig. 14. Bifurcation diagram of K_1 versus x.

by choosing $K_2 = 0.9$. We also can convert the chaotic motion to period-2 and period-4 for a suitable K_2.

5.8. Controlling chaos by optimal control

Optimal control is a well-established engineering control strategy, and is useful for both linear and non-linear system with linear or non-linear controllers [6]. Now, we use a typical optimal control for a chaos control. We consider Eq. (5.7) with a controller u and define the Hamilton

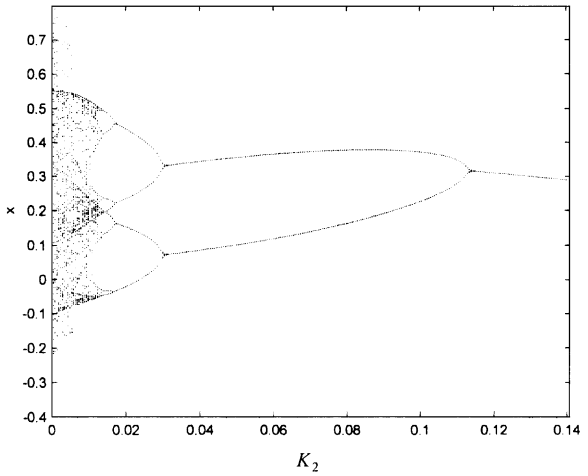

Fig. 15. Bifurcation diagram of K_2 versus x.

function:

$$H(x,y,z,u,p) = P^{\mathrm{T}}F(x,y,z,u,t), P^{\mathrm{T}} = [p_1p_2p_3].$$

Following the variation principle of optimal control, we can obtain

$$p_1y + p_2\,[dz^2\cos x + \tfrac{1}{2}(e + pz^2)\sin 2x - \sin x - by] = 0, \tag{5.8}$$

$$-p_2(2dz\cos x + pz\sin 2x) = 0. \tag{5.9}$$

This yields a non-trivial solution for (p_1, p_2) if and only if

$$2dz\cos x + pz\sin 2x = 0. \tag{5.10}$$

It gives an optimal surface singularly in the state space. This type of control assumes values on the two allowable boundaries (5.8) alternatively according to a switching surface. Locating system trajectories on the surface, a typical feedback control in the form

$$u = -k_b\,\mathrm{sgn}[2dz\cos x + pz\sin 2x]$$

can be used. By adjusting the value of k_b in the above controller with the signum function

$$sign[v] = \begin{cases} 1 & \text{if } v > 0, \\ 0 & \text{if } v = 0, \\ -1 & \text{if } v < 0, \end{cases}$$

the chaotic motion can be controlled to periodic motion which we desired by the bifurcation diagram as shown in Fig. 15.

6. Conclusions

The dynamic system of the rotational machine with centrifugal governor exhibits a rich variety of non-linear behaviors as certain parameters varied. Due to the effect of non-linearity, regular or

chaotic motions may occur. In this paper, both analytical and computational methods have been employed to study the dynamical behaviors of the non-linear system.

The conditions of stability and instability of fixed points have been determined by using the Lyapunov direct method. The periodic and chaotic motions of the non-autonomous system are obtained by the numerical methods such as power spectrum, Poincaré map and Lyapunov exponents. All these phenomena have been displayed in bifurcation diagrams. More information on the behaviors of the periodic and the chaotic motion can be found in parametric diagrams. The changes of parameters play a major role for the nonlinear system. Chaotic motion is the motion which has a sensitive dependence on initial condition in deterministic physical systems. The chaotic motion has been detected by using the Lyapunov exponents and Lyapunov dimensions. In spite of the fact that these methods are different, the results obtained matches each other.

The presence of chaotic behavior is generic for suitable non-linearities, ranges of parameters and external force, where one wishes to avoid or control so as to improve the performance of a dynamical system. Eight methods are used to control chaos effectively. Especially, we can control the chaotic motion to any assigned periodic motion by addition of period force, periodic impulse control, the delayed feedback control, external force feedback control, optimal control and adaptive control algorithm. For our system, the delayed feedback control is the best method compared with the others.

References

[1] S. Wiggins, Introduction to Applied Nonlinear Dynamical Systems and Chaos, Springer, New York, 1990.
[2] J. Guckenheimer, P.J. Holmes, Nonlinear Oscillations of Dynamical Systems and Bifurcations of Vector Fields, Springer, New York, 1983.
[3] S. Wiggins, Global Bifurcations and Chaos, Springer, New York, 1988.
[4] H.K. Khalil, Nonlinear Systems, 2nd edition, Prentice-Hall, Englewood Cliffs, NJ, 1996.
[5] K. Pyragas, Continuous control of chaos by self-controlling feedback, Physics Letters A 170 (1992) 421–428.
[6] G. Chen, X. Dong, From Chaos to Order: Methodologies, Perspectives and Applications, World Scientific, Singapore, 1998.
[7] B.A. Huberman, E. Lumer, Dynamics of adaptive system, IEEE Transactions on Circuits and Systems 37 (1990) 547–550.